Supplement of Atmos. Chem. Phys., 22, 13739–13752, 2022
https://doi.org/10.5194/acp-22-13739-2022-supplement

Atmospheric Chemistry and Physics Open Access

Supplement of

Potential underestimation of ambient brown carbon absorption based on the methanol extraction method and its impacts on source analysis

Zhenqi Xu et al.

Correspondence to: Mingjie Xie (mingjie.xie@colorado.edu, mingjie.xie@nuist.edu.cn)

Text S1. Calculations of the coefficient of divergence and average relative percent difference

The coefficient of divergence (COD) used earlier comparing PM component concentrations at pairs of sampling sites (Wongphatarakul et al., 1998) was calculated to show the degree of uniformity between collocated measurements of solvent extract absorption, and is defined as

$$\mathrm{COD}_{12} = \sqrt{\frac{1}{n}\sum_{i=1}^{n}\left(\frac{x_{i1}-x_{i2}}{x_{i1}+x_{i2}}\right)^2} \quad (1)$$

where x_{i1} and x_{i2} represent the light-absorbing property of i^{th} sample from Sampler I and II, and n is the size of paired samples. COD values approaching 0 and 1 indicate no and maximum difference between collocated measurements, and a COD value of 0.2 was used to define a significant heterogeneity (Wilson et al., 2005; Krudysz et al., 2008). The average relative percent difference (ARPD, %) was calculated as an estimate of fractional uncertainty from collocated measurement data, and is defined as

$$\mathrm{ARPD} = \frac{2}{n}\sum_{i=1}^{n}\frac{|x_{i1}-x_{i2}|}{(x_{i1}+x_{i2})} \times 100\% \quad (2)$$

Text S2. PMF data preparation and factor number determination

Similar to Xie et al. (2022), 102 observations of 9 $PM_{2.5}$ bulk components (NH_4^+, SO_4^{2-}, NO_3^-, Ca^{2+}, Mg^{2+}, OC, EC, WSOC and MEOC) and 50 OMMs (22 *n*-alkanes, 14 PAHs, 5 steranes and hopanes, C5-alkanetriols, 2-methyltetrols, levoglucosan, and 6 sugar and sugar alcohols) were selected to apportion the light absorption of aerosol extracts in methanol ($Abs_{365,m}$) and the solvent with the highest extraction efficiency (η) to sources. The measurement results of the bulk components in $PM_{2.5}$ and total OMMs (gas + particle phase) are summarized in Table S3. Uncertainty fractions of bulk components and aerosol extract absorption were set to their ARPD values of collocated Q_f-Q_b data (Yang et al., 2021; Xie et al., 2022; Figure 1). The uncertainties of OMM

concentrations were calculated as (Zhang et al., 2009; Xie et al., 2016, 2019; Liu et al., 2017)

$$\text{Uncertainty}=\sqrt{(20\%\times \text{concentration})^2+(0.5\times \text{detection limit})^2} \quad (3)$$

Missing values and measurements below detection limits (BDL) were replaced by the geometric mean of all observations and half of the detection limit, respectively. Their accompanying uncertainties were set to four times the geometric mean and five-sixths the detection limit (Polissar et al., 1998).

Because the identified sources for BrC absorption are essential, interpretability is the primary basis for determining an appropriate factor number and is defined by how PMF apportioned specific source-related OMMs (Shrivastava et al., 2007). Furthermore, the change in Q/Q_{exp} with varying factor numbers is also a typical indicator of factor number selection (Liu et al., 2017; Wang et al., 2017, 2018). Specifically, Q/Q_{exp} is expected to change less dramatically when the factor number increases to a certain value. The EPA PMF5.0 tool can evaluate the robustness of individual base-case solutions with three built-in error estimation methods, including bootstrapping (BS), displacement (DISP), and BS-DISP (Norris et al., 2014; Paatero et al., 2014; Brown et al., 2015). In this work, 100 BS runs were conducted with a minimum *r* value of 0.8 (default 0.6) to map the BS run to base run factors. Once the error code or swap counts at dQmax=4 of DISP analysis were not 0, the base case solution was considered invalid. All input species were included for BS-DISP analysis.

In Table S4, Q/Q_{exp} changes by 9.14% from 8- to 10-factor solutions, less significant than the value (10.0%–15.1%) for factor numbers varying from 4 to 8, indicating that a factor number of eight is needed to explain the input data. When examining the factor profiles, the 8-factor solution had the most interpretable factor profiles by identifying a lubricating oil combustion factor (Figure S8). The 9-factor

solution resolved an unexplainable factor characterized by a mixture of anthropogenic and natural source markers (e.g., steranes, Ca^{2+}, and saccharides). In comparison to the input data set for PMF analysis in Xie et al. (2022), this work replaces the light absorption of water extracts with DMF extracts at 365 nm ($Abs_{365,d}$). The error estimation results of these two studies were similar. Although the factor matching rate of the BS runs decreased as the factor number increased, the BS matching rate of the 8-factor solution was larger than 50% when the default minimum *r* value (0.6) was used. Furthermore, no DISP swap was observed and the acceptance rates of BS-DISP analysis were higher than 50% for 4- to 10-factor solutions. Therefore, the resulting base-case solutions are valid and interpretable, and an 8-factor solution was finalized to explain the sources of aerosol extract absorption.

Table S1. $PM_{2.5}$ sampling information for solvent test and concentrations of bulk carbon fractions (μg m^{-3}).

Sampling date	Sampling Periods	ΔM (μg m^{-3}) [a]	OC1	OC2	OC3	OC4	EC1	EC2	EC3	OC[b]	EC[c]
One-time extraction (*N* = 11)											
2019/12/3	8:00 a.m.–7:00 p.m.	95.2	0.55 ± 0.20[d]	2.17 ± 0.20	3.17 ± 0.32	2.46 ± 0.12	1.98 ± 0.32	0.55 ± 0.14	0.17 ± 0.34	8.36 ± 0.69	2.70 ± 0.48
2019/12/4	8:00 a.m.–7:00 p.m.	68.1	0.32 ± 0.052	1.90 ± 0.044	2.85 ± 0.072	2.35 ± 0.074	1.85 ± 0.20	0.49 ± 0.18	0.028 ± 0.14	7.42 ± 0.13	2.36 ± 0.47
2019/12/7	8:00 p.m. –7:00 a.m.	98.9	1.07 ± 0.11	3.20 ± 0.07	4.38 ± 0.30	3.44 ± 0.13	2.55 ± 0.43	0.46 ± 0.20	0.35 ± 0.35	12.1 ± 0.36	3.36 ± 0.74
2019/12/8	8:00 a.m.–7:00 p.m.	87.2	0.79 ± 0.07	2.74 ± 0.18	3.51 ± 0.34	2.69 ± 0.21	2.37 ± 0.60	0.44 ± 0.020	0.22 ± 0.25	9.72 ± 0.39	3.03 ± 0.57
2019/12/8	8:00 p.m. –7:00 a.m.	71.9	0.76 ± 0.091	2.87 ± 0.17	3.87 ± 0.14	3.23 ± 0.081	2.23 ± 0.49	0.37 ± 0.20	0.28 ± 0.35	10.7 ± 0.45	2.88 ± 0.93
2019/12/9	8:00 a.m.–7:00 p.m.	81.6	0.58 ± 0.026	2.87 ± 0.084	4.08 ± 0.076	3.51 ± 0.19	2.31 ± 0.37	0.40 ± 0.11	0.37 ± 0.37	11.0 ± 0.31	3.08 ± 0.52
2019/12/9	8:00 p.m. –7:00 a.m.	76.4	0.91 ± 0.090	3.65 ± 0.15	5.12 ± 0.087	4.41 ± 0.34	2.90 ± 0.56	0.62 ± 0.31	0.73 ± 0.17	14.1 ± 0.15	4.25 ± 0.89
2019/12/19	8:00 p.m. –7:00 a.m.	69.6	0.60 ± 0.18	2.36 ± 0.11	2.66 ± 0.032	2.28 ± 0.081	2.64 ± 0.22	0.46 ± 0.12	0.098 ± 0.23	7.90 ± 0.35	3.19 ± 0.14
2019/12/20	8:00 a.m.–7:00 p.m.	93.7	0.65 ± 0.22	2.30 ± 0.060	2.77 ± 0.065	2.30 ± 0.075	1.87 ± 0.21	0.54 ± 0.32	0.30 ± 0.33	8.02 ± 0.41	2.71 ± 0.83
2019/12/21	8:00 p.m. –7:00 a.m.	81.5	0.66 ± 0.096	2.24 ± 0.15	2.49 ± 0.15	1.95 ± 0.11	1.77 ± 0.12	0.62 ± 0.23	0.23 ± 0.29	7.34 ± 0.45	2.62 ± 0.56
2019/12/22	8:00 a.m.–7:00 p.m.	62.1	0.41 ± 0.055	3.31 ± 0.18	1.98 ± 0.28	1.62 ± 0.064	1.13 ± 0.064	0.21 ± 0.066	/	7.32 ± 0.45	1.33 ± 0.14
Two-time extraction (*N* = 10)											
2019/12/10	8:00 a.m.–7:00 p.m.	93.8	0.66 ± 0.067	3.44 ± 0.15	5.18 ± 0.15	4.25 ± 0.066	2.30 ± 0.11	0.35 ± 0.061	0.20 ± 0.050	13.5 ± 0.35	2.84 ± 0.13
2019/12/10	8:00 p.m. –7:00 a.m.	120	1.86 ± 0.092	4.25 ± 0.13	8.64 ± 0.39	7.49 ± 0.62	3.86 ± 0.35	0.28 ± 0.053	0.15 ± 0.12	22.2 ± 0.29	4.29 ± 0.49
2019/12/11	8:00 a.m.–7:00 p.m.	119	0.67 ± 0.097	3.39 ± 0.13	5.94 ± 0.39	4.99 ± 0.026	2.68 ± 0.093	0.38 ± 0.036	0.22 ± 0.17	15.0 ± 0.51	3.28 ± 0.21
2019/12/11	8:00 p.m. –7:00 a.m.	86.5	0.93 ± 0.13	3.08 ± 0.19	4.28 ± 0.24	3.15 ± 0.056	1.96 ± 0.21	0.29 ± 0.11	0.21 ± 0.18	11.4 ± 0.60	2.45 ± 0.45
2019/12/12	8:00 a.m.–7:00 p.m.	83.3	0.64 ± 0.015	2.50 ± 0.095	3.59 ± 0.060	2.44 ± 0.20	1.82 ± 0.18	0.67 ± 0.091	0.30 ± 0.12	9.17 ± 0.28	2.79 ± 0.33
2019/12/15	8:00 a.m.–7:00 p.m.	71.7	0.29 ± 0.092	2.13 ± 0.085	2.77 ± 0.072	1.96 ± 0.13	1.33 ± 0.14	0.82 ± 0.11	0.59 ± 0.20	7.15 ± 0.29	2.74 ± 0.44
2019/12/15	8:00 p.m. –7:00 a.m.	60.5	0.35 ± 0.079	1.98 ± 0.19	2.18 ± 0.10	1.74 ± 0.19	1.01 ± 0.047	0.25 ± 0.11	0.22 ± 0.37	6.24 ± 0.49	1.47 ± 0.46
2019/12/16	8:00 a.m.–7:00 p.m.	81.1	0.41 ± 0.026	2.70 ± 0.11	3.53 ± 0.12	2.80 ± 0.14	2.03 ± 0.11	0.45 ± 0.035	0.15 ± 0.16	9.43 ± 0.39	2.63 ± 0.23
2019/12/16	8:00 p.m. –7:00 a.m.	65.2	0.35 ± 0.021	2.31 ± 0.090	2.82 ± 0.098	2.49 ± 0.17	1.71 ± 0.10	0.21 ± 0.079	0.12 ± 0.17	7.97 ± 0.35	2.04 ± 0.31
2019/12/17	8:00 a.m.–7:00 p.m.	66.2	0.41 ± 0.21	1.82 ± 0.21	2.23 ± 0.11	2.23 ± 0.078	2.02 ± 0.044	0.25 ± 0.079	0.10 ± 0.13	6.76 ± 0.44	2.37 ± 0.24

[a] ΔM = difference between pre- and post-weigh mass of each filter sample (μg)/sample volume (m^3); [b] OC = OC1 + OC2 + OC3 + OC4; [c] EC = EC1 + EC2 + EC3; [d] average ± standard deviation derived from three times analysis.

Table S2. Species information of the 25-PAH mixture.

Compound Name (Formula)	Abbreviation	MW
naphthalene ($C_{10}H_8$)	NAP	128
2-methylnaphthalene ($C_{11}H_{10}$)	2-MeNAP	142
1-methylnaphthalene ($C_{11}H_{10}$)	1-MeNAP	142
biphenyl ($C_{12}H_{10}$)	BP	154
acenaphthene ($C_{12}H_{10}$)	ACE	154
acenaphthylene ($C_{12}H_8$)	ACY	152
fluorene ($C_{13}H_{10}$)	FLU	166
2,6-dimethylnaphthalene ($C_{12}H_{12}$)	2,6-DMN	156
2,3,5-trimethylnaphthalene ($C_{13}H_{14}$)	2,3,5-TMNAP	170
dibenzothiophene ($C_{12}H_8S$)	DBT	184
phenanthrene ($C_{14}H_{10}$)	PHE	178
anthracene ($C_{14}H_{10}$)	ANT	178
1-methylphenanthrene ($C_{15}H_{12}$)	1-MePHE	192
fluoranthene ($C_{16}H_{10}$)	FLT	202
pyrene ($C_{16}H_{10}$)	PYR	202
benz[a]anthracene ($C_{18}H_{12}$)	BaA	228
chrysene ($C_{18}H_{12}$)	CHY	228
benzo[b]fluoranthene ($C_{20}H_{12}$)	BbF	252
benzo[k]fluoranthene ($C_{20}H_{12}$)	BkF	252
benz[e]pyrene ($C_{20}H_{12}$)	BeP	252
benz[a]pyrene ($C_{20}H_{12}$)	BaP	252
perylene ($C_{20}H_{12}$)	PER	252
indeno[1,2,3-cd]pyrene ($C_{22}H_{12}$)	IDP	276
benzo[ghi]perylene ($C_{22}H_{12}$)	BghiP	276
dibenz[ah]anthracene ($C_{22}H_{14}$)	DahA	278

Table S3. Input species data for PMF analysis of BrC absorption from Xie et al. (2022).

	No. of Obs.	Median	Mean ± stdev	Range
Light absorption coefficients (Mm^{-1})				
$Abs_{365,m}$[a]	109	5.59	6.43 ± 4.66	0.38 – 29.6
Bulk components ($\mu g\ m^{-3}$)				
WSOC	109	4.20	4.45 ± 2.13	1.22–10.3
MEOC[b]	109	5.82	6.22 ± 2.53	1.93 – 12.9
OC	109	7.03	7.82 ± 3.36	2.15–16.7
EC	109	2.82	2.97 ± 1.10	1.01–5.91
ammonium (NH_4^+)	109	4.04	4.98 ± 3.26	1.14–21.5
nitrate (NO_3^-)	109	9.48	11.7 ± 10.4	0.12–53.0
sulfate (SO_4^{2-})	109	7.73	8.89 ± 4.24	2.87–21.6
calcium (Ca^{2+})	109	1.58	1.93 ± 1.45	0.080–6.87
magnesium (Mg^{2+})	108	0.11	0.13 ± 0.097	0.0048–0.45
Organic molecular markers (OMMs, $ng\ m^{-3}$)				
n-Alkanes				
dodecane (n-C12)	102	36.7	38.4 ± 17.7	5.76 – 95.4
tridecane (n-C13)	102	35.8	37.6 ± 14.6	12.9 – 88.1
pentadecane (n-C15)	102	36.3	38.7 ± 15.0	10.6 – 81.6
hexadecane (n-C16)	102	29.4	32.1 ± 17.0	5.23 – 104
heptadecane (n-C17)	102	22.8	25.7 ± 15.5	3.96 – 83.0
octadecane (n-C18)	102	15.2	16.0 ± 8.60	3.82 – 47.8
eicosane (n-C20)	102	7.43	8.45 ± 4.72	1.30 – 27.6
henicosane (n-C21)	102	6.94	7.47 ± 3.55	1.47 – 21.3
docosane (n-C22)	102	6.54	7.23 ± 4.74	0.60 – 33.1
tricosane (n-C23)	102	6.69	8.14 ± 5.69	1.68 – 41.2
tetracosane (n-C24)	102	5.31	7.19 ± 5.51	1.75 – 39.1
pentacosane (n-C25)	102	7.18	8.32 ± 5.16	1.94 – 36.2
hexacosane (n-C26)	102	4.12	4.82 ± 3.11	1.00 – 22.3
heptacosane (n-C27)	102	5.52	6.10 ± 3.40	1.24 – 17.8
octacosane (n-C28)	102	2.99	3.15 ± 2.04	0.25 – 13.8
nonacosane (n-C29)	102	6.33	9.26 ± 8.86	0.92 – 47.2
triacontane (n-C30)	101	1.88	2.05 ± 1.44	0.083 – 9.29
hentriacontane (n-C31)	102	4.62	5.78 ± 3.99	0.76 – 23.6
dotriacontane (n-C32)	102	1.45	1.59 ± 0.83	0.34 – 5.15
tritriacontane (n-C33)	102	2.76	3.62 ± 3.02	0.77 – 21.5
tetratriacontane (n-C34)	102	1.58	1.80 ± 1.13	0.16 – 8.63
pentatriacontane (n-C35)	101	0.96	1.18 ± 0.78	0.25 – 4.98
PAHs				
naphthalene (NAP)	102	75.2	92.5 ± 56.7	16.7 – 299
2-methylnaphthalene (2-MeNAP)	102	21.3	24.6 ± 13.7	4.91 – 66.0
dimethylnaphthalene-156-sum[e] (ISO-156-SUM)	102	17.2	25.0 ± 18.2	4.07 – 78.7
trimethylnaphthalene-170-sum[f] (ISO-170-SUM)	102	10.3	14.5 ± 10.8	0.96 – 47.8
phenanthrene (PHE)	102	10.1	12.8 ± 8.54	0.90 – 40.2
fluoranthene (FLT)	102	5.02	6.30 ± 4.36	1.08 – 20.2
pyrene (PYR)	102	2.06	2.86 ± 2.25	0.38 – 10.9
benz[a]anthracene (BaA)	102	0.52	0.94 ± 1.08	0.080 – 6.97
chrysene/triphenylene (CHY/TP)	102	1.03	1.41 ± 1.24	0.20 – 7.93
benzo[b&k]fluoranthene (BbkF)	102	0.86	1.21± 1.09	0.14 – 6.29
benz[e]pyrene (BeP)	102	0.8	1.05 ± 0.94	0.10 – 5.55
benz[a]pyrene (BaP)	102	0.69	0.89 ± 0.74	0.13 – 4.68
indeno[1,2,3-cd]pyrene (IDP)	102	0.83	1.04 ± 0.69	0.14 – 3.44
benzo[ghi]perylene (BghiP)*	102	0.88	1.15 ± 0.88	0.13 – 4.66

[a] Light absorption coefficients of methanol extracts at 365 nm; [b] methanol-extractable OC.

Table S3. Continue

	No. of Obs.	Median	Mean ± stdev	Range
Steranes and Hopanes				
aaa-20R-cholestane (aaa-CHO)	102	2.07	2.42 ± 1.76	0.33 – 10.7
abb-20R 24S-methylcholestane (abb-MeCHO)	102	0.58	0.68 ± 0.47	0.10 – 2.84
aaa-20R 24R-ethylcholestane (aaa-EtCHO)	102	0.77	0.97 ± 0.64	0.16 – 3.22
17a(H),21b(H)-30-norhopane (NorHOP)	102	1.02	1.13 ± 0.78	0.11 – 5.38
17a(H),21b(H)-hopane (HOP)	102	0.77	0.86 ± 0.54	0.083 – 3.72
Isoprene SOA tracers				
C5-alkene triols	104	0.96	14.5 ± 43.7	0.022 – 319
2-Methyltetrols	104	1.72	10.8 ± 19.1	0.031 – 111
Anhydro sugar				
levoglucosan	104	45	64.8 ± 71.0	0.016 – 415
Sugars and sugar alcohols				
fructose	104	3.22	14.7 ± 62.3	0.0057 – 473
mannose	103	0.33	0.42 ± 0.32	0.0034 – 1.62
glucose	104	7.52	14.0 ± 31.0	0.11 – 239
xylitol	93	0.82	0.89 ± 0.63	0.036 – 3.15
arabitol	103	5.16	7.29 ± 7.00	0.026 – 39.3
mannitol	103	6.95	11.3 ± 11.6	0.10 – 74.2

Table S4. Summaries of BS, DISP and BS-DISP error estimation diagnostics and Q/Q_{exp} values from 4- to 10-factor PMF solutions.

	4-factor	5-factor	6-factor	7-factor	8-factor	9-factor	10-factor
BS diagnostics							
Lowest %BS mapping	83	66	47	34	30	37	29
Highest % unmapped	17	34	51	53	65	62	67
DISP diagnostics							
Error Code:	0	0	0	0	0	0	0
Largest Decrease in Q:	0	-0.061	-0.27	-2.55	-0.12	-0.77	-0.23
%dQ:	0	-0.0004	-0.0022	-0.023	-0.0013	-0.0093	-0.0031
Highest swaps by factor:	0	0	0	0	0	0	0
BS-DISP Diagnostics							
Number of cases accepted	84	76	77	54	68	61	56
% of cases accepted	84%	76%	77%	54%	68%	61%	56%
Largest decrease in Q	-134	-63.4	1069	1225	-995	-252	-500
%dQ	-0.74	-0.42	8.65	11.3	-10.5	-3.04	-6.82
Number of decreases in Q	14	20	18	13	19	11	14
Number of swaps in best fit	0	0	0	22	4	17	10
Number of swaps in DISP	2	4	5	11	9	11	20
Highest swaps by factor:	1	1	2	0	2	16	7
Q/Qexp	3.51	2.98	2.48	2.19	1.97	1.79	1.63

Table S5. Light absorbance (A_λ) of authentic standard compounds at specific wavelengths (λ).

	A_{300}	A_{350}	A_{365}	A_{400}	A_{450}	A_{500}	A_{550}
			4-Nitrophenol (1.90 ng μL^{-1})				
Water	0.11 ± 0.0023	0.071 ± 0.0013	0.039 ± 0.0004	0.015 ± 0.0015	0.0010 ± 0.00	0	0
MeOH	0.14 ± 0.0030	0.042 ± 0.0005	0.019 ± 0.0012	0.0072 ± 0.0019	0	0	0
MeOH/DCM (1:1)	0.14 ± 0.0052	0.060 ± 0.0018	0.029 ± 0.0028	0.016 ± 0.0060	0.0012 ± 0.0008	0	0
MeOH/DCM (1:2)	0.14 ± 0.0086	0.061 ± 0.0031	0.025 ± 0.0015	0.0060 ± 0.0029	0.0008 ± 0.0004	0	0
THF	0.17 ± 0.0022	0.022 ± 0.0011	0.0084 ± 0.0005	0.0006 ± 0.0005	0	0	0
DMF	0.10 ± 0.0044	0.048 ± 0.0023	0.022 ± 0.0004	0.058 ± 0.0086	0.10 ± 0.013	0	0
			4-Nitrocatechol (1.84 ng μL^{-1})				
Water	0.043 ± 0.0064	0.064 ± 0.0055	0.058 ± 0.0024	0.039 ± 0.014	0.028 ± 0.017	0.0042 ± 0.0022	0
MeOH	0.056 ± 0.0015	0.077 ± 0.0019	0.060 ± 0.0015	0.014 ± 0.0007	0.0034 ± 0.0005	0	0
MeOH/DCM (1:1)	0.060 ± 0.0015	0.083 ± 0.0013	0.070 ± 0.0012	0.020 ± 0.0034	0.0058 ± 0.0033	0	0
MeOH/DCM (1:2)	0.059 ± 0.0036	0.082 ± 0.0047	0.069 ± 0.0038	0.020 ± 0.0026	0.0064 ± 0.0025	0	0
THF	0.063 ± 0.0013	0.083 ± 0.0016	0.055 ± 0.0013	0.0036 ± 0.0005	0	0	0
DMF	0.030 ± 0.0015	0.032 ± 0.0044	0.032 ± 0.0043	0.046 ± 0.0013	0.20 ± 0.016	0.011 ± 0.0005	0
			PAHs mixture (0.024 ng $\mu L^{-1,a}$)				
MeOH	0.11 ± 0.0029	0.024 ± 0.0011	0.026 ± 0.0009	0.014 ± 0.0007	0.0014 ± 0.0005	0	0
MeOH/DCM (1:1)	0.12 ± 0.0046	0.026 ± 0.011	0.028 ± 0.0012	0.013 ± 0.0007	0.0014 ± 0.0005	0	0
MeOH/DCM (1:2)	0.013 ± 0.0027	0.027 ± 0.0008	0.029 ± 0.0005	0.013 ± 0.0004	0.0016 ± 0.0005	0	0
THF	0.13 ± 0.0098	0.026 ± 0.0019	0.028 ± 0.0022	0.011 ± 0.0009	0.0010 ± 0.00	0	0
DMF	0.14 ± 0.0044	0.027 ± 0.0012	0.030 ± 0.0009	0.011 ± 0.0009	0.0014 ± 0.0005	0	0
			PAHs mixture (0.0080 ng $\mu L^{-1,a}$)				
MeOH	0.032 ± 0.011	0.0072 ± 0.0004	0.0072 ± 0.0004	0.0042 ± 0.0004	0	0	0
MeOH/DCM (1:1)	0.041 ± 0.0028	0.0080 ± 0.0007	0.0090 ± 0.0007	0.0042 ± 0.0004	0	0	0
MeOH/DCM (1:2)	0.045 ± 0.0023	0.0088 ± 0.0008	0.0092 ± 0.0008	0.0040 ± 0.0007	0	0	0
THF	0.043 ± 0.0022	0.0084 ± 0.0005	0.0092 ± 0.0004	0.0038 ± 0.0004	0	0	0
DMF	0.042 ± 0.0015	0.0072 ± 0.0004	0.0082 ± 0.0004	0.0022 ± 0.0004	0	0	0

[a] Concentration of each species in the 25-PAH mixture.

Table S6. Light absorption coefficients at 365 nm (Abs_{365}, Mm^{-1}) of collocated Q_f and Q_b sample extracts in DMF.

	Sampler I				Sampler II			
	No. of obs.	Median	Mean ± std	Range	No. of obs.	Median	Mean ± std	Range
				Q_f				
Abs_{365}	100	7.63	8.58 ± 5.12	1.14–23.3	104	6.64	8.55 ± 5.49	1.14–31.1
				Q_b				
Abs_{365}	56	0.70	0.69 ± 0.49	0.33–2.86	69	0.38	0.62 ± 0.46	0.33–3.15

Table S7. Comparisons between PMF estimations of DMF and MeOH extract absorption, bulk carbon components and artifact-corrected measurement data.

	Observation		PMF estimation		PMF estimation vs. observed data
	Median	Mean ± stdev	Median	Mean ± stdev	y: Observation
$Abs_{365,d}$	7.03	8.26 ± 4.89	7.14	7.54 ± 3.81	y = 1.13x - 0.28 (r = 0.88)
$Abs_{365,m}$	5.59	6.24 ± 4.11	4.64	5.57 ± 3.79	y = 0.94x + 1.02 (r = 0.86)
WSOC	4.11	4.38 ± 2.04	3.99	4.33 ± 1.79	y = 1.10x - 0.37 (r = 0.96)
MEOC	5.81	6.15 ± 2.45	5.98	6.17 ± 2.36	y = 0.99x + 0.053 (r = 0.95)
OC	7.03	7.75 ± 3.25	7.49	7.82 ± 3.13	y = 1.01x - 0.15 (r = 0.97)
EC	2.79	2.95 ± 1.09	2.82	2.88 ± 1.02	y = 0.95x + 0.21 (r = 0.88)
WSIIs[a]+OC+EC	34.3	38.5 ± 19.1	32.4	36.1 ± 15.8	y = 1.19x – 4.40 (r = 99)

[a] Water-soluble inorganic ions, including NH_4^+, NO_3^-, SO_4^{2-}, Ca^{2+}, and Mg^{2+}.

Table S8. Average relative contributions (%) of individual factors to Abs_{365} of DMF and MeOH extracts and bulk components.

Factors	Biomass burning	Non-combustion fossil	Lubricating oil combustion	Coal combustion	Dust resuspension	Biogenic emission	Isoprene oxidation	Secondary inorganics
$Abs_{365,d}$	34.5	10.9	3.33	11.1	23.2	0.04	11.9	5.00
$Abs_{365,m}$	47.7	3.20	6.40	19.2	20.7	0	0	2.84
WSOC	27.2	5.12	8.07	0.00	27.4	5.25	17.4	9.61
MEOC	20.2	6.78	11.9	1.82	27.3	7.29	16.4	8.39
OC	20.3	5.92	9.71	2.46	31.2	9.70	13.6	7.12
EC	18.6	8.40	12.7	5.26	22.7	12.1	8.37	11.9
WSII+OC+EC	20.9	3.79	7.57	7.45	14.9	5.89	9.63	29.8

Figure S1

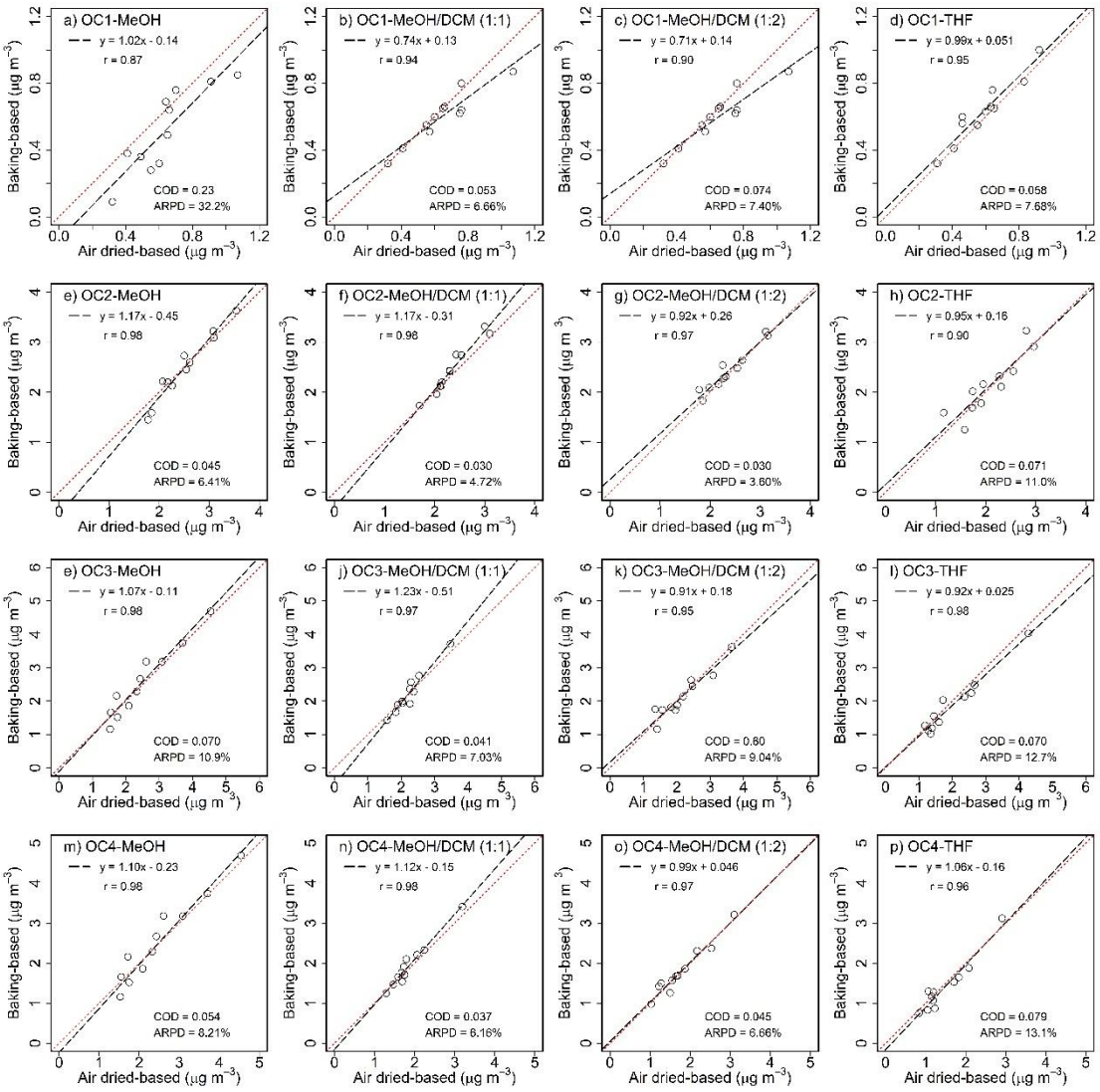

Figure S1. Comparisons of extracted OC fractions based on rOC measurements after air-dried and baking processes with the one-time extraction procedure.

Figure S2

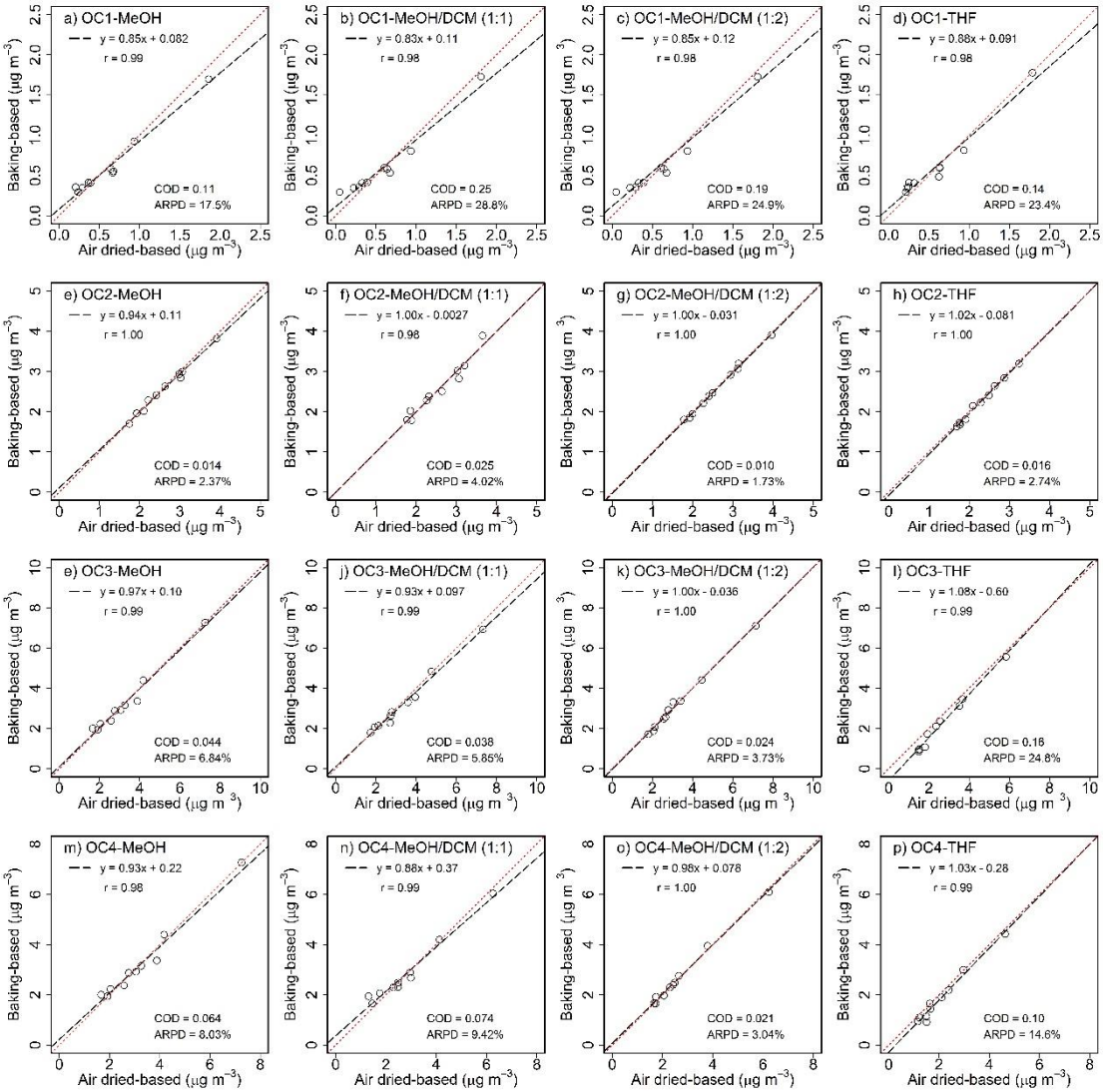

Figure S2. Comparisons of extracted OC fractions based on rOC measurements after air-dried and baking processes with the two-time extraction procedure.

Figure S3

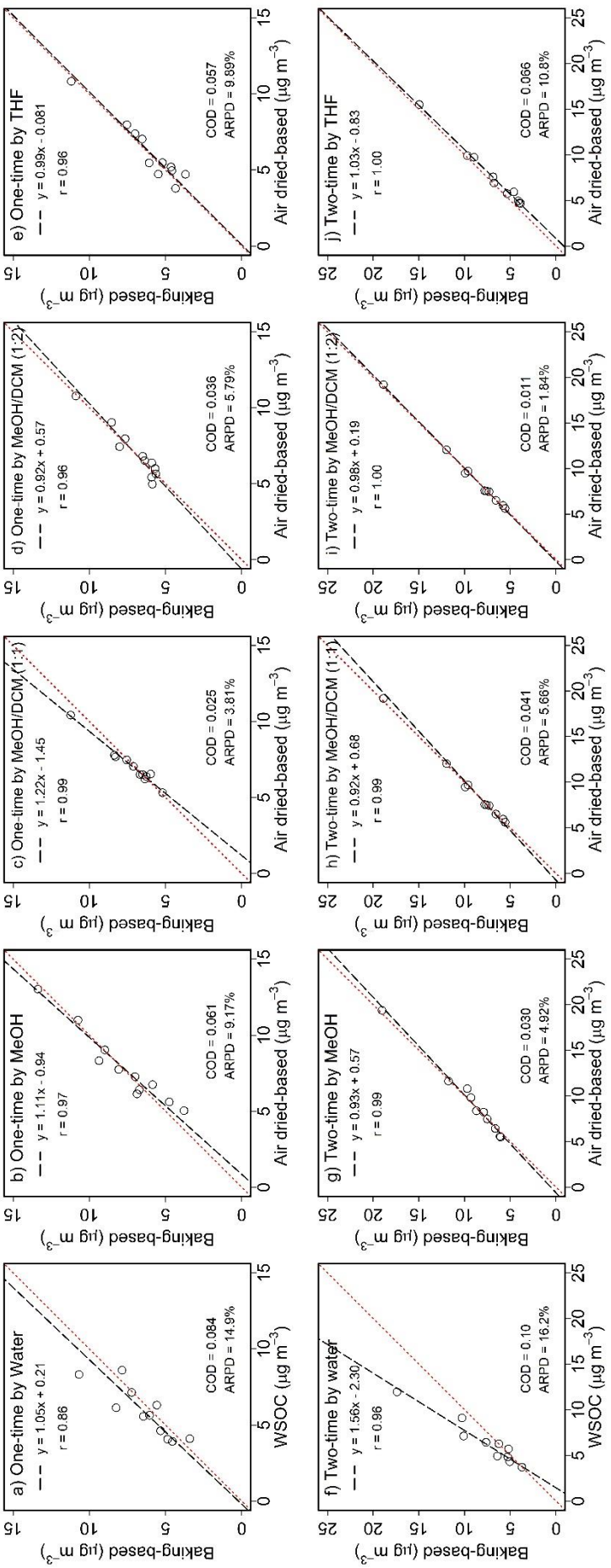

Figure S3. Comparisons of total SEOC based on rOC measurements after air-dried and baking processes for (a-e) one-time extraction and (f-j) two-time extraction procedures. The SEOC of water was determined by measuring WSOC in water extracts and rOC in the extracted filter after the baking process, respectively.

Figure S4

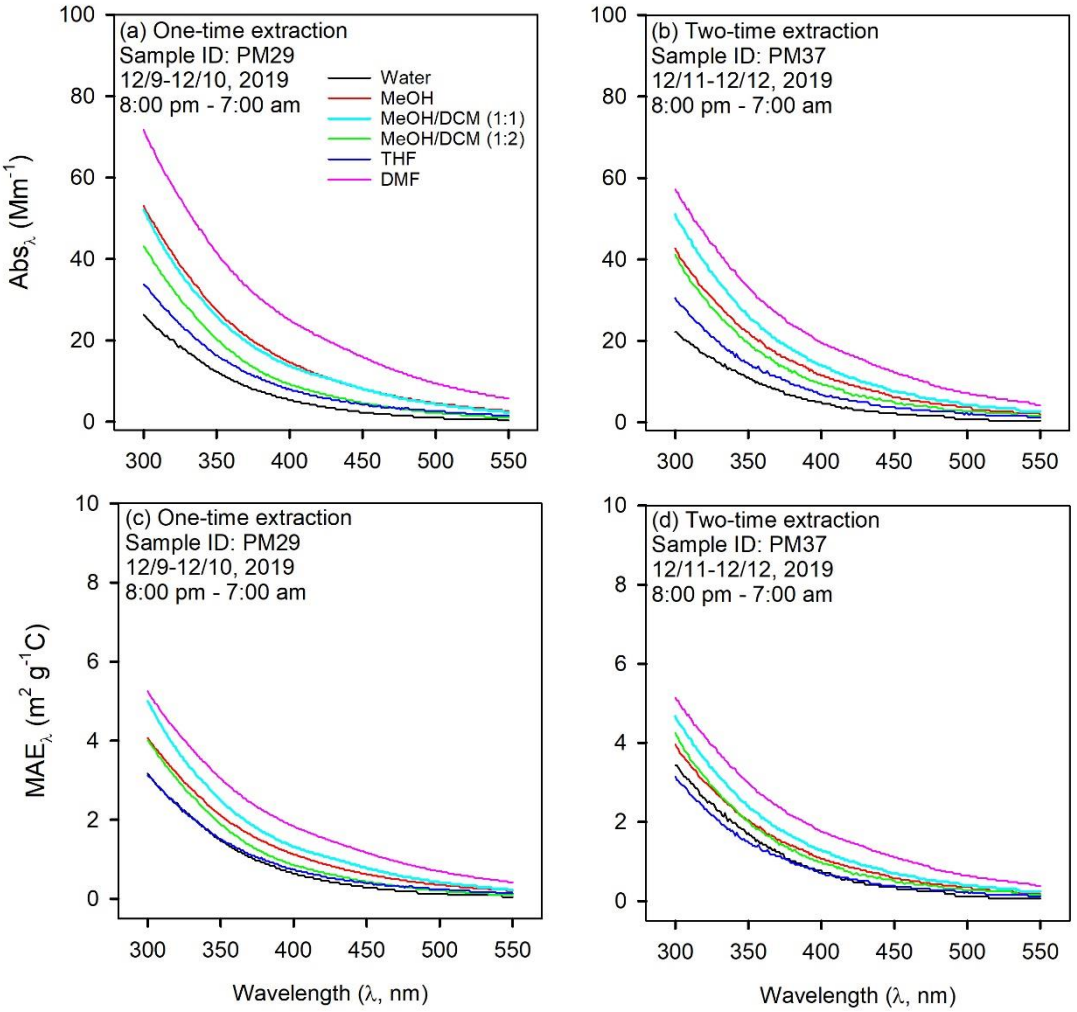

Figure S4. Abs$_\lambda$ and MAE$_\lambda$ spectra of (a, c) sample PM29 with one-time extraction and (b, d) sample PM37 with two-time extraction.

Figure S5

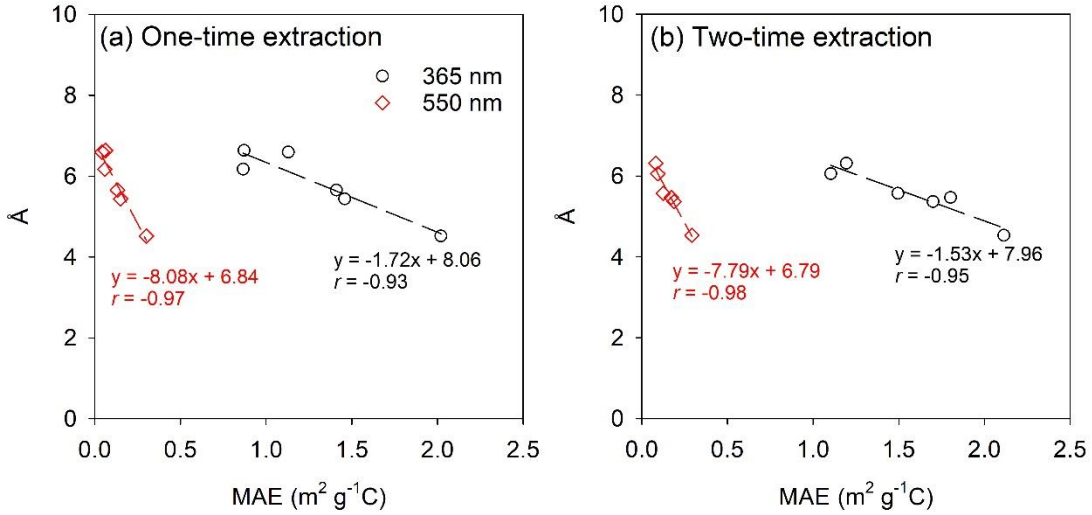

Figure S5. Linear relationships of average Å versus $MAE_{365/550}$ of individual solvent extracts in Table 2.

Figure S6

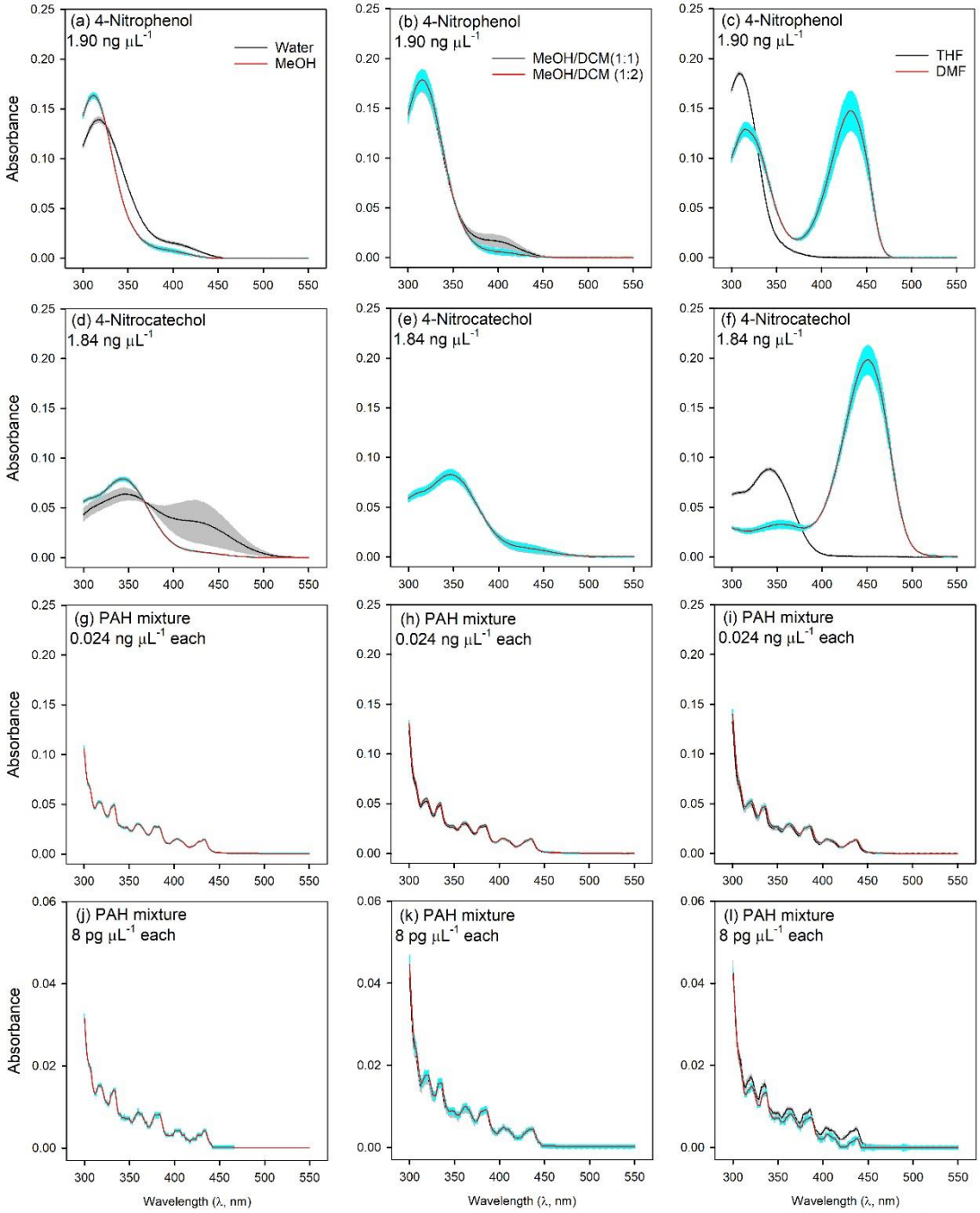

Figure S6. UV/Vis spectra (300 – 550 nm) of (a-c) 4-nitrophenol at 1.90 ng μL^{-1}, (d-f) 4-nitrocatechol at 1.84 ng μL^{-1}, and (g-i) 25 PAH mixtures at 0.024 ng $\mu L^{-1}$and (j-l) 8 pg μL^{-1} for each species in the five solvents and solvent mixtures.

Figure S7

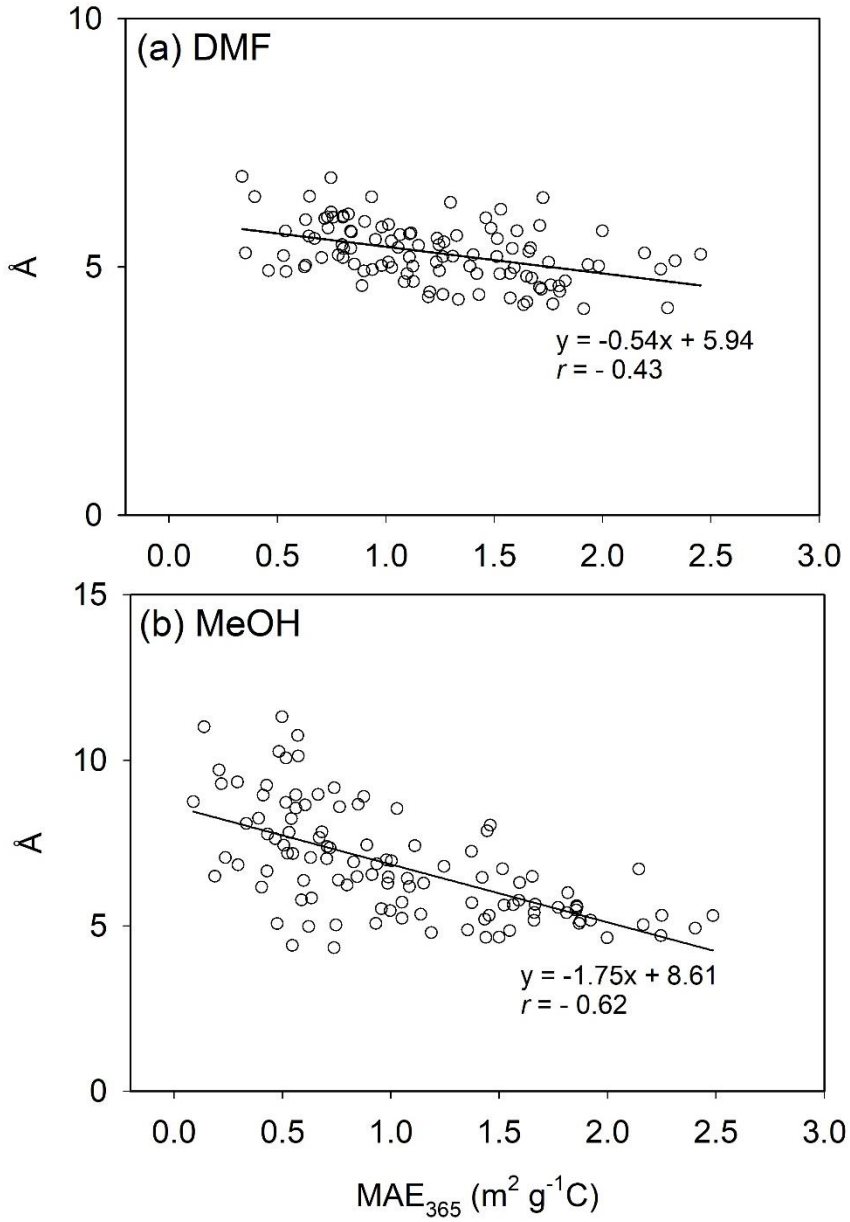

Figure S7. Linear relationships of $Å_d$ versus $MAE_{365, d}$ and $Å_m$ versus $MAE_{365, m}$ based on averages of duplicate Q_f–Q_b data.

Figure S8

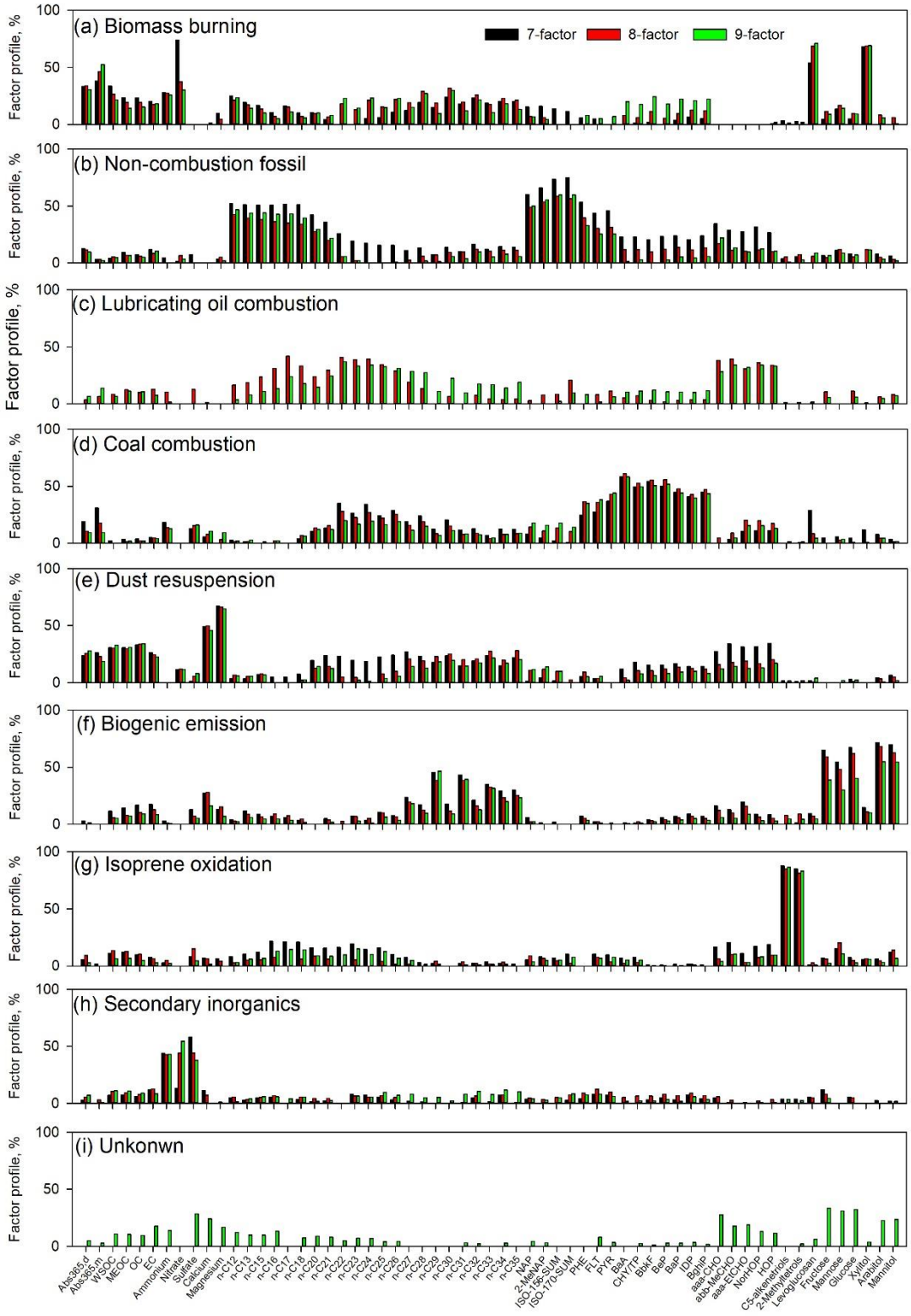

Figure S8. Normalized factor profiles of 7-, 8-, and 9-factor PMF solutions.

Figure S9

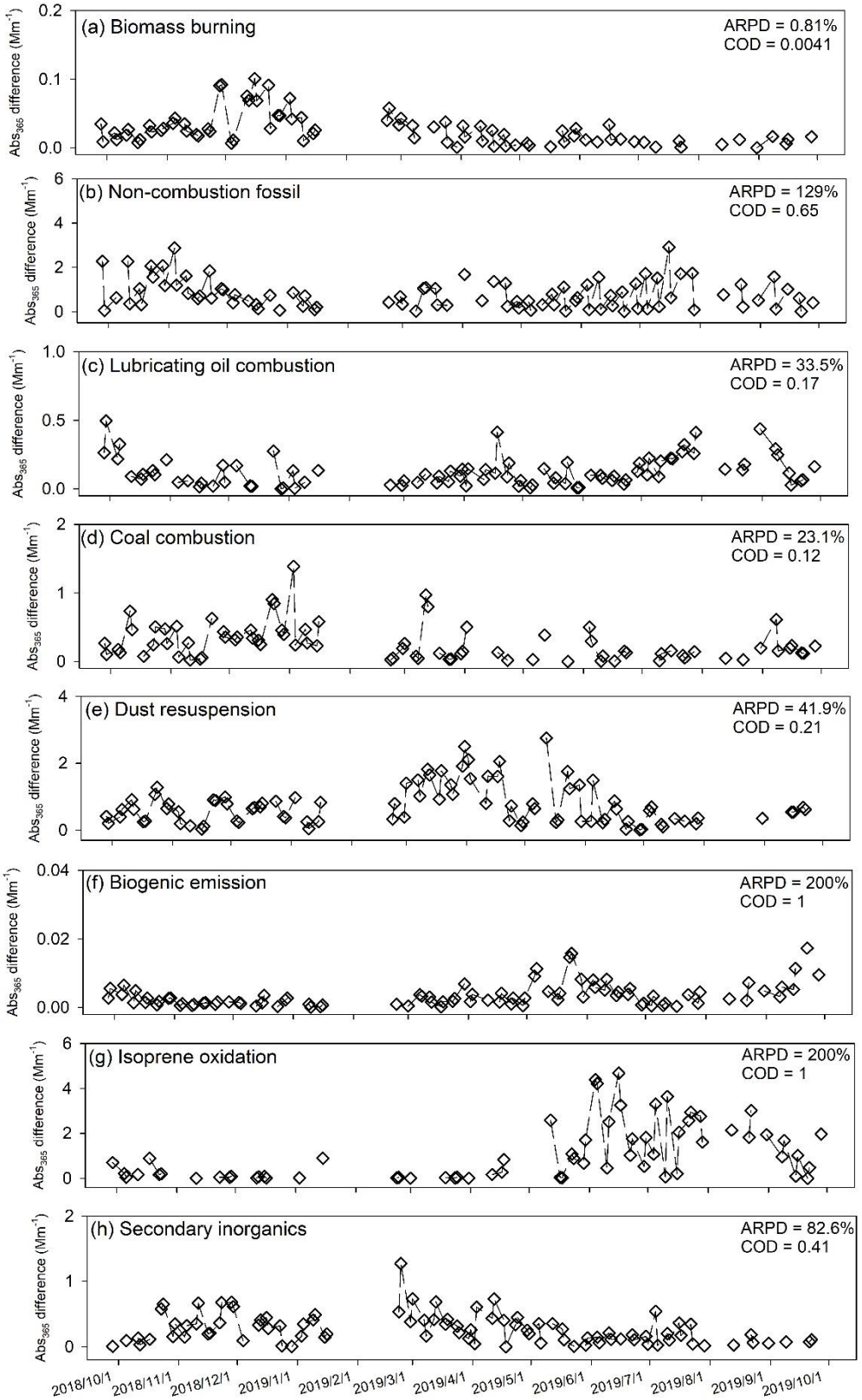

Figure S9. Time series of the absolute difference in factor contributions to Abs_{365} of DMF and MeOH extracts.

References

Brown, S. G., Eberly, S., Paatero, P., and Norris, G. A.: Methods for estimating uncertainty in PMF solutions: Examples with ambient air and water quality data and guidance on reporting PMF results, Sci. Total Environ., 518-519, 626-635, https://doi.org/10.1016/j.scitotenv.2015.01.022, 2015.

Krudysz, M. A., Froines, J. R., Fine, P. M., and Sioutas, C.: Intra-community spatial variation of size-fractionated PM mass, OC, EC, and trace elements in the Long Beach, CA area, Atmos. Environ., 42, 5374-5389, 10.1016/j.atmosenv.2008.02.060, 2008.

Liu, B., Wu, J., Zhang, J., Wang, L., Yang, J., Liang, D., Dai, Q., Bi, X., Feng, Y., Zhang, Y., and Zhang, Q.: Characterization and source apportionment of PM2.5 based on error estimation from EPA PMF 5.0 model at a medium city in China, Environ. Pollut., 222, 10-22, https://doi.org/10.1016/j.envpol.2017.01.005, 2017.

Norris, G., Duvall, R., Brown, S., and Bai, S. J. I., Petaluma: EPA positive matrix factorization (PMF) 5.0 fundamentals and user guide prepared for the us environmental protection agency office of research and development, Washington, DC, 2014.

Paatero, P., Eberly, S., Brown, S., and Norris, G.: Methods for estimating uncertainty in factor analytic solutions, Atmos. Meas. Tech., 7, 781, 2014.

Polissar, A. V., Hopke, P. K., and Paatero, P.: Atmospheric aerosol over Alaska - 2. Elemental composition and sources, J. Geophys. Res. Atmos., 103, 19045-19057, 10.1029/98jd01212, 1998.

Shrivastava, M. K., Subramanian, R., Rogge, W. F., and Robinson, A. L.: Sources of organic aerosol: Positive matrix factorization of molecular marker data and comparison of results from different source apportionment models, Atmos. Environ., 41, 9353-9369, 10.1016/j.atmosenv.2007.09.016, 2007.

Wang, Q., He, X., Huang, X. H., Griffith, S. M., Feng, Y., Zhang, T., Zhang, Q., Wu, D., and Yu, J. Z.: Impact of secondary organic aerosol tracers on tracer-based source apportionment of organic carbon and PM2. 5: a case study in the pearl river delta, China, ACS Earth Space Chem., 1, 562-571, 2017.

Wang, Q., Qiao, L., Zhou, M., Zhu, S., Griffith, S., Li, L., and Yu, J. Z.: Source apportionment of PM2.5 using hourly measurements of elemental tracers and major constituents in an urban environment: Investigation of time-resolution influence, J. Geophys. Res. Atmos., 123, 5284-5300, 10.1029/2017JD027877, 2018.

Wilson, J. G., Kingham, S., Pearce, J., and Sturman, A. P.: A review of intraurban variations in particulate air pollution: Implications for epidemiological research, Atmos. Environ., 39, 6444-6462, 10.1016/j.atmosenv.2005.07.030, 2005.

Wongphatarakul, V., Friedlander, S. K., and Pinto, J. P.: A Comparative study of PM2.5 ambient aerosol chemical databases, Environ. Sci. Technol., 32, 3926-3934, 10.1021/es9800582, 1998.

Xie, M., Mladenov, N., Williams, M. W., Neff, J. C., Wasswa, J., and Hannigan, M. P.: Water soluble organic aerosols in the Colorado Rocky Mountains, USA: composition, sources and optical properties, Sci. Rep., 6, 39339, 10.1038/srep39339, 2016.

Xie, M., Chen, X., Holder, A. L., Hays, M. D., Lewandowski, M., Offenberg, J. H., Kleindienst, T. E., Jaoui, M., and Hannigan, M. P.: Light absorption of organic carbon and its sources at a southeastern U.S. location in summer, Environ. Pollut., 244, 38-46, https://doi.org/10.1016/j.envpol.2018.09.125, 2019.

Xie, M., Peng, X., Shang, Y., Yang, L., Zhang, Y., Wang, Y., and Liao, H.: Collocated measurements of light-absorbing organic carbon in PM2.5: Observation uncertainty and organic tracer-based source apportionment, J. Geophys. Res. Atmos., 127, e2021JD035874, https://doi.org/10.1029/2021JD035874, 2022.

Yang, L., Shang, Y., Hannigan, M. P., Zhu, R., Wang, Q. g., Qin, C., and Xie, M.: Collocated speciation of PM2.5 using tandem quartz filters in northern nanjing, China: Sampling artifacts and measurement uncertainty, Atmos. Environ., 246, 118066, https://doi.org/10.1016/j.atmosenv.2020.118066, 2021.

Zhang, Y., Sheesley, R. J., Schauer, J. J., Lewandowski, M., Jaoui, M., Offenberg, J. H., Kleindienst, T. E., and Edney, E. O.: Source apportionment of primary and secondary organic aerosols using positive matrix factorization (PMF) of molecular markers, Atmos. Environ., 43, 5567-5574, 10.1016/j.atmosenv.2009.02.047, 2009.